JOURNAL OF MATERIALS SCIENCE 26 (1991) 6706–6714

Low temperature degradation of Y–TZP materials

J. J. SWAB
US Army Materials Technology Laboratory, Watertown, MA 02172, USA

Seven yttria–tetragonal zirconia polycrystal (TZP) materials were examined to determine if they were susceptible to low temperature degradation. Flexure specimens were exposed to approximately 800 Pa of water vapour pressure for 50 h between 200 and 400 °C. Only one of the TZPs was unaffected by these low temperature treatments. Three underwent catastrophic degradation after all the low temperature treatments, while the final three had property losses of varying degrees, depending on the treatment temperature.

1. Introduction

Yttria–tetragonal zirconia polycrystal (Y–TZP) materials are candidates for structural applications because of an unusual combination of high strength and toughness. These excellent properties stem from a stress-assisted "martensitic" transformation of a metastable tetragonal (t) phase to the stable monoclinic (m) phase. It is believed that absorption of the crack tip energy by the t–grains in the vicinity of the crack tip causes the transformation resulting in enhanced properties. Other mechanisms such as crack tip deflection and microcracking may also contribute to this enhancement.

Although Y–TZPs have these excellent properties they suffer from a low temperature (150–400 °C) degradation phenomenon. Kobayashi *et al.* [1] were the first to observe this degradation. Since then, many additional studies [2–17] have been initiated to examine further this phenomenon. Their general observations can be summarized as follows:

1. the degradation is most pronounced between 200 and 300 °C.
2. the degradation results in large decreases in strength, toughness and density, and a significant increase in the m–ZrO_2 content.
3. the degradation is due to the $t \rightarrow m$ transformation which is accompanied by micro- and macrocracking.
4. the $t \rightarrow m$ transformation initiates on the surface and proceeds into the bulk.
5. the $t \rightarrow m$ transformation is slowed by a decrease in grain size and/or an increase in the stabilizer content.
6. the $t \rightarrow m$ transformation is greatly enhanced by the presence of water or water vapour.

Theories based on the interaction between the ZrO_2–Y_2O_3 and H_2O have been put forth to explain the rapid, low-temperature degradation of Y–TZP materials. Sato *et al.* [5] have proposed a theory where Zr–OH bonds are formed when water reacts with Zr–O–Zr bonds at the crack tip. They have shown that in addition to aqueous solutions, certain nonaqueous solutions with a lone-pair electron orbital opposite a proton donor site, enhance the rate of $t \rightarrow m$ transformation at low temperatures. It was concluded that under these conditions the strain which acts to stabilize the tetragonal phase may be released and this, coupled with the growth of preexisting flaws, accelerates the transformation.

The hypotheses of Yoshimura *et al.* [10, 13] is similar in that it is also based on the formation of Zr–OH bonds but they suggest a four-step degradation process. The H_2O is adsorbed onto the Y–TZP surface and dissociates forming Zr–OH bonds which creates stress sites. The stresses build as the OH^- ions diffuse through the surface and the lattice resulting in nucleation sites for the phase transformation. When the stress build-up reaches a critical level, the $t \rightarrow m$ transformation will occur with the associated micro- and macrocracking enabling the process to continue into the bulk. Their assumptions are based on findings which show that the transformed m–ZrO_2 has an OH^- group which is not found in the untransformed t–ZrO_2, the addition of the OH^- group to the monoclinic phase increases the lattice parameter, and the lattice parameter can be returned to its original value if the specimen is dried.

Lange *et al.* [7] have seen the formation of 20–50 nm crystallites of α–$Y(OH)_3$ and proposed that the formation of this hydroxide draws yttria from the tetragonal grains on the surface creating monoclinic nuclei. Growth of the nuclei continues with further yttria depletion until it reaches a critical size where it can spontaneously grow, transforming the tetragonal grains to monoclinic. If the transformed grains are large enough, microcracking will occur. The microcracking provides an avenue for the water to penetrate to subsurface grains allowing the process to repeat. If the transformed grains are smaller than the critical size required for microcracking, then the transformation and subsequent degradation will be limited by the long-range diffusion of yttria to the surface. Work by Winnubst and Burggraaf [8] using Auger electron spectroscopy has shown a homogeneous

0022–2461/91 $03.00 + .12

yttrium-rich surface layer on specimens after only 5 h of exposure to 177 °C in a nitrogen environment. This clearly supports the theory of Lange and his co-workers.

The theories reviewed here are based on observations and at this time are still speculative. Other potential theories should not be ruled out and further work is still needed to detail the mechanisms of this low-temperature degradation.

The purpose of this study was to determine whether several commercial and experimental Y–TZP materials are affected by low-temperature annealing in the presence of water vapour.

2. Experimental procedure

Y–TZP materials were obtained from a variety of manufacturers which are listed in Table I. These materials differ only slightly in yttria content and grain size but the differences proved to be important, as will be shown. Type "B" bars ($3 \times 4 \times 50$ mm) were machined from billets of these materials according to MIL STD 1942 (MR). Due to material limitations the AC Sparkplug TZP–110 was machined into "A" ($1.5 \times 2 \times 30$ mm) as well as type "B" bars, according to the same standard. The bars were then divided into four groups with each group undergoing one of the following treatments: Zero hours at 200 °C (as-received); 50 h at 200 °C with $\approx$ 800 Pa water vapour pressure; 50 h at 300 °C with $\approx$ 800 Pa water vapour pressure and 50 h at 400 °C with $\approx$ 800 Pa water vapour pressure. Due to material limitations the AC Sparkplug material was only subjected to the first two treatments.

Treatments were done in an autoclave apparatus consisting of a 1-litre pressure vessel, a furnace, temperature controller, timer, pressure gauge and power supply. Bars were placed in the pressure vessel on a stainless steel wire mesh screen which minimized obstacles to heat flow and maintained uniformity throughout the test. The pressure was kept constant by varying the amount of water placed in the vessel prior to the start of the test.

The bulk density was measured by the Archimedes technique. Room temperature strength was determined from a minimum of 10 bars for each material per condition (except where noted) using 4-point bending, according to MIL STD 1942 (MR), with inner and outer spans of 20 and 40 mm for the type "B" bars, and 10 and 20 mm for type "A" at a cross-head speed of 0.5 mm min^{-1} for both. The fracture surface of each bar was examined optically using a low magnification microscope in an attempt to determine the cause of failure. In several cases, a scanning electron microscope (SEM) was used to improve the chances of determining the flaw type.

The presence and amount of zirconia phases in each material was determined using X-ray diffraction with CuK_α radiation over an angular range of 25–40° 2Θ. The surface volume fraction of monoclinic and tetragonal-plus-cubic zirconia was calculated using equations and constants [18] that take into account the difficulty in deconvoluting the tetragonal (1 0 1) and cubic (1 1 1) peaks.

3. Results

3.1. Observations

Physical changes were quite obvious in four of the seven materials after the three treatments, which included water vapour. All of the TOSH and all but two bars of the KY, fractured into several pieces due to the 200 °C treatment, as seen in Fig. 1(b). Subsequent treatments at 300 and 400 °C resulted in more severe degradation of all the bars of both of these TZPs (Fig. 1(c)). Low power ($\simeq$ 25x) optical examination of the surfaces of the remaining pieces of each material showed extensive macrocracking as seen in Fig. 2. Micro- and macrocracking have been reported [2–6, 9, 11, 13] to be common indicators of the occurrence of the $t \rightarrow m$ transformation in this phenomenon.

One of the general observations of this degradation phenomenon is that the $t \rightarrow m$ transformation and accompanying micro- and macrocracking initiate on the surface and proceed into the bulk. This implies

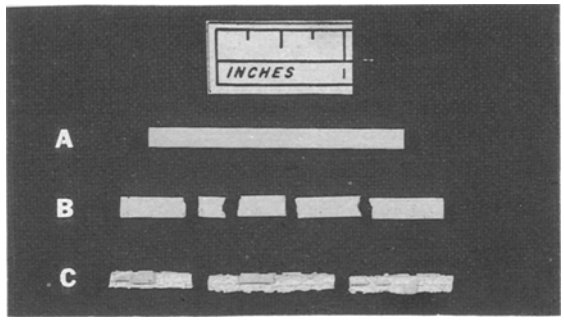

Figure 1 A is the TOSH and KY in the as-received state; B is after 50 h at 200 °C with $\approx$ 800 Pa water vapour pressure; C is after 50 h at 300 or 400 °C with $\approx$ 800 Pa water vapour pressure.

TABLE I Evaluated materials

	Code	Manufacturer	Material	Process	Mol % Y_2O_3	Mean grain size (μm)[19]
Japanese	KY	Kyocera	Z-201	Sintered	2.8	0.65
	TOSH	Toshiba	TASZIC	Sintered	2.3	0.49
	HIT	Hitachi	1985	Hot-Pressed	2.0	0.37
	NGK	NGK Locke	Z-191	Sintered	3.0	0.18
	KS	Koransha	1986	Sintered	3.0	0.50
	KH	Koransha	1986	HIP'ed	3.0	0.41
Domestic	AC	AC Sparkplug	TZP-110	Sintered	2.6	0.80

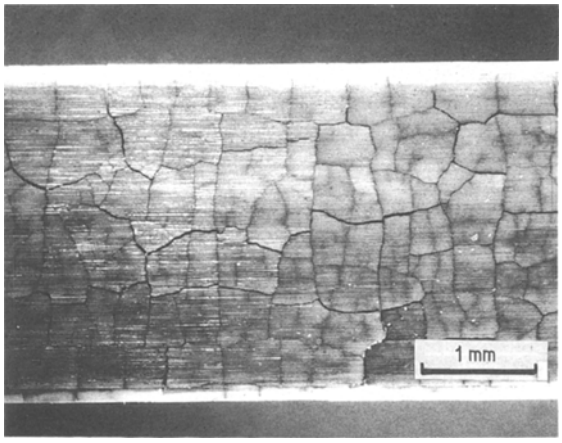

Figure 2 Optical photograph of macrocracks on the surface of TOSH, AC and KY TZPs.

that a larger volume of material requires longer exposure times before disintegration occurs than the same material in a much smaller volume, exposed to identical conditions. This is the case with the AC material. Both type "A" and "B" bars were exposed to 200°C with water vapour for 50 h. The "A" bars completely disintegrated (Fig. 3(c)) but the "B" bars (Fig. 3(a)) remained intact.

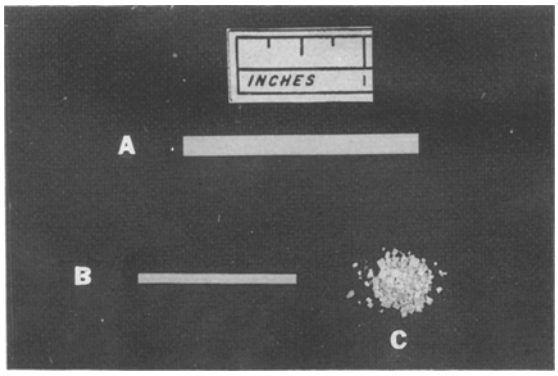

Figure 3 A is the AC type "B" bar in the as-received state and after 50 h at 200 °C with ≈ 800 Pa water vapour pressure; B is the AC type "A" bar in the as-received state; C, the "A" bar, is after 50 h at 200 °C with ≈ 800 Pa water vapour pressure.

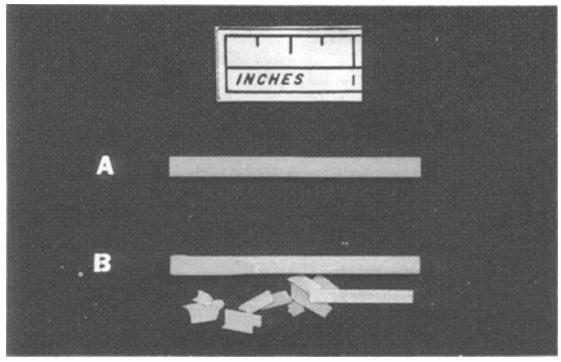

Figure 4 A is the HIT in the as-received state and after 50 h at 300 or 400 °C with ≈ 800 Pa water vapour pressure; B is after 50 h at 200 °C with ≈ 800 Pa water vapour pressure.

The fourth material that underwent physical change was the HIT at 200 °C with water vapour. As seen in Fig. 4, entire sides of a bar spalled off in sheets of relatively uniform thickness. This spalling did not occur after the treatments at higher temperatures. The number of sides which spalled off varied with each bar. They ranged in thickness from 250 to 650 μm. Schmauder and Schubert [9] and Yoshimura *et al.* [13] have seen large cracks running parallel to the surface of the specimen. It is believed that the crack separates the transformed material from the untransformed material. The former study measured the thickness of the degraded layer in a 2.0 mol % Y–TZP exposed for 1000 h at 250 °C in air, as approximately 100 μm. The difference in thickness and crack severity can be attributed to the presence of water vapour during the treatment used in the present study, because it has been shown that the presence of water enhances the $t \rightarrow m$ transformation [5, 12–14, 16]. The remaining Y–TZPs showed no signs of physical change.

3.2. Density and modulus of elasticity

Table II summarizes the changes in density and modulus of elasticity. It can be seen from the data that the density of the TOSH, AC and KY TZPs decreased between 2 and 6% due to the treatments. A fourth

TABLE II

		Material	KY	AC	TOSH	HIT	KS	KH	NGK
Property		Units							
Density:	Company Listing	gcc^{-1}	5.9	NDA	6.05	6.08	6.05	NDA	5.91
	As-received		5.93	5.95	5.96	6.15	5.93	6.13	5.80
	50 h at 200 °C w/H_2O		5.68	5.87	5.86	5.92	5.87	6.03	5.88
	50 h at 300 °C w/H_2O		5.59	*****	5.81	5.98	5.92	6.08	5.84
	50 h at 400 °C w/H_2O		5.56	*****	5.78	6.09	6.07	5.97	5.97
Sonic MOE:	Company Listing	GPa	206	NDA	180	209	NDA	NDA	205
	As-received		201	204	200	213	210	214	208
	50 h at 200 °C w/H_2O		192	201	---	203	210	214	207
	50 h at 300 °C w/H_2O		---	*****	---	213	211	214	207
	50 h at 400 °C w/H_2O		---	*****	---	212	211	214	208

****–not used in this test.
---degradation too severe to determine values.
NDA–no data available.

TZP, HIT, decreased approximately 4% after the 200 °C treatment, but only 1% and < 1% after treatment at 300 and 400 °C, respectively. Watanabe [2] have seen similar changes in density, but in a 4 mol % yttria stabilized zirconia. The density of the remaining materials is unaffected by the treatments.

Corresponding to the density decrease is a proportional decrease in the modulus of elasticity (MOE) of the KY and HIT after the 200 °C treatment. The MOE of the TOSH and AC, and the KY after the 300 and 400 °C treatments, could not be determined due to the severe degradation of the bars.

3.3. Phase stability

The change in surface m–ZrO_2 content with heat treatment temperature is shown in Fig. 5. With the exception of NGK, all other TZPs showed dramatic increases in the surface m–ZrO_2 content. The TOSH, AC and KY all had 200% increases in surface m–ZrO_2 after all heat treatment temperatures. HIT had an increase from 10% to almost 80% after the 200 and 300 °C treatments, but after 400 °C, the m–ZrO_2 content increased to just over 20%. The KH also had a dramatic initial increase from ≈ 15% to ≈ 80%, but only 60% and 42% after the 300 and 400 °C treatments, respectively. The KS TZP showed a 500–700% increase after all treatments. Many investigators [2–6, 11–14, 16, 17] have seen similar increases in the amount of monoclinic phase when zirconia stabilized with 2–4 mol % yttria is subjected to low temperature treatments (200 – 400 °C) in the presence of water.

3.4. Strength*

Three of the five TZPs which could be used for flexure strength testing showed significant strength degradation as a result of the treatments, as shown in Fig. 6.

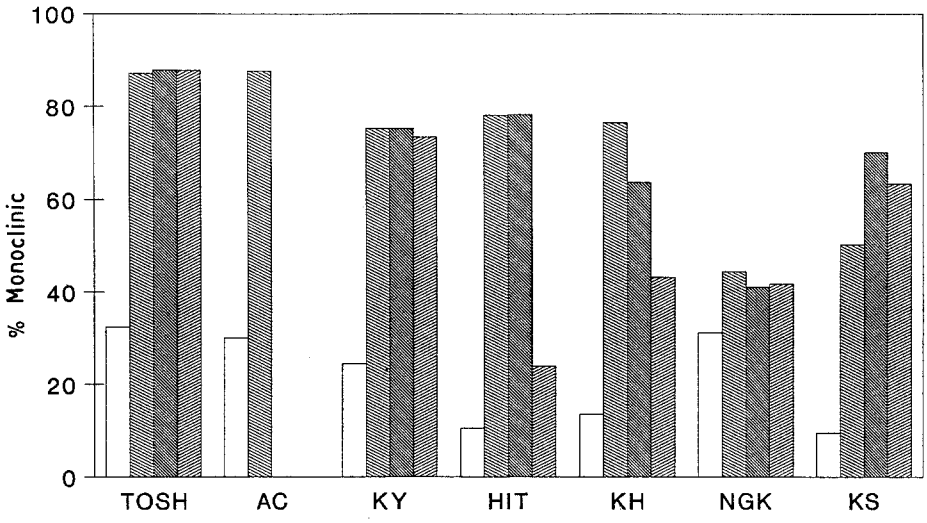

Figure 5 Change in the surface monoclinic content after 50 h at varying temperature with ≈ 800 Pa water vapour pressure where □ is as-received, ▨ 200 °C, ▨ 300 °C and ▨ 400 °C.

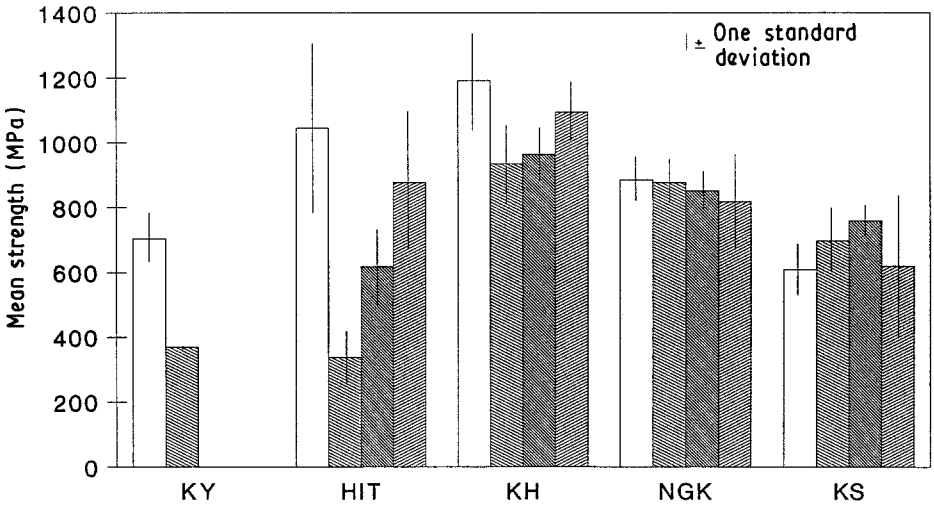

Figure 6 Change in room temperature strength after 50 h at varying temperature with ≈ 800 Pa water vapour pressure where □ is as-received, ▨ 200 °C, ▨ 300 °C and ▨ 400 °C.

*Although size "B" bars of the AC material survived the 200 °C treatment, a strength comparison could not be made since the as-received strength was determined with "A" size bars only. Nevertheless, the "B" bars were broken in 4-point bending to determine the location of the failure origin and the depth of transformation.

For example, the strength of KY after the 200 °C treatment was approximately 50% less than for the as-received condition. This amount of loss is similar to that after exposure to 1000 °C for 500 h [19].

The HIT and KH both showed a similar trend in strength degradation, in that the degradation was most severe during the 200 °C treatment and gradually decreased as the treatment temperature increased. However, the degradation was more pronounced in HIT, as it lost 68, 41 and 16% of its room temperature strength with each increase in temperature, while the KH lost only 22, 16 and 8% for the same treatments, respectively.

The percentage of strength degradation reported here is in excellent agreement with that published by Watanabe *et al.* [2] and Sato *et al.* [12, 16] for zirconias stabilized with 2–5 mol % yttria subjected to similar test conditions.

Although NGK and KS did show slight fluctuations in strength with the treatments, these changes were well within experimental error. This indicates that the strength of both materials was essentially unaffected by the treatment.

3.5. Fractography

Analysis of the fracture surface of the as-received bars of all the TZPs showed that the strength-limiting flaws tended to be porosity related (i.e., pore, porous region, etc.) but other flaw types such as large grain(s), inclusions and machining damage were also observed. Examination after treatments revealed that in several instances the flaw location rather than the flaw type changed.

In the AC material, as shown in Fig. 7(a), there is a surface layer which is believed to be m–ZrO_2, that has been transformed from the tetragonal phase due to the treatment. This m–ZrO_2 layer is approximately 100–150 μm deep around the entire bar. Other investigators [4, 6, 12, 13, 16, 17] have also reported seeing these zones of transformation. The strength-limiting flaw is still porosity related (Fig. 7(b)) but it is located in the t–ZrO_2, just inside the interface which separates the two phases. For the two KY bars which survived the 200 °C treatment, the zone of transformation was ≈ 300 μm deep and expanded to ≈ 600 μm around the chamfers of the bar (Fig. 8). Macrocracking can be seen to penetrate approximately 50 μm into the m–ZrO_2 zone. The microcracking in conjunction with the large m–ZrO_2 transformation zone, is the probable cause of failure since there is no evidence of a single-strength limiting flaw on the fracture surface.

Fractography of the HIT after the 200 °C treatment was difficult because it was very easy to remove sheets of material which had not spalled off during the treatment. Fig. 9(a) is a low-power (≈ 20x) photo of the fracture surface of a bar in which three sides remained intact. The interface between the untransformed t–ZrO_2 and the m–ZrO_2 surface layers is easily seen but the strength-limiting flaw is not obvious. Fig. 9(b) shows a pore located at the junction of the t–ZrO_2 material and two sections of the m–ZrO_2 layer, one of which is no longer attached to the bar. Cracks can be seen running parallel to the interface and the higher magnification photo (Fig. 9(c)) shows the build up of layers within the m–ZrO_2 zone and extensive microcracking. Examination after the subsequent treatments showed a large reduction in the size of the transformation zone to ≈ 50 μm after the 300 °C treatment, and to 15–20 μm after the 400 °C treatment (Fig. 9(d) and (e)). There is microcracking associated with the m–ZrO_2 zone in Fig. 9(d) but none is evident in Fig. 9(e).

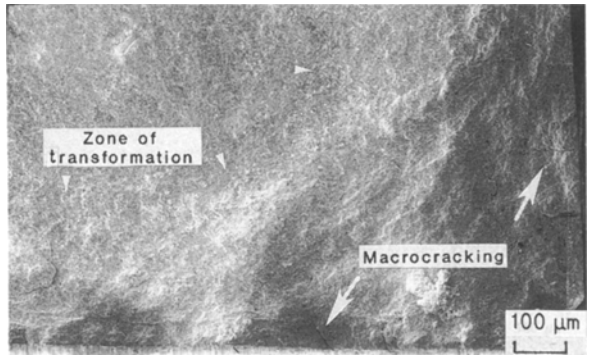

Figure 8 SEM photo of the fracture surface of a KY bar after 50 h at 200 °C with ≈ 800 Pa water vapour pressure showing the depth of the transformation zone and the associated macrocracking.

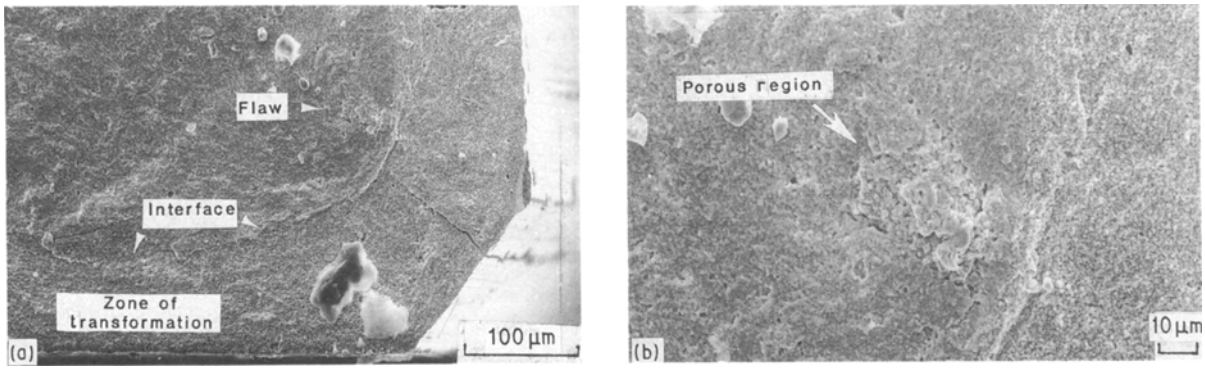

Figure 7 (a) SEM photo of the fracture surface of an AC bar after 50 h at 200 °C with ≈ 800 Pa water vapour pressure showing the depth of the transformation zone and the flaw location (× 230); (b) SEM photo of the strength limiting flaw – porous region – in the same AC bar.

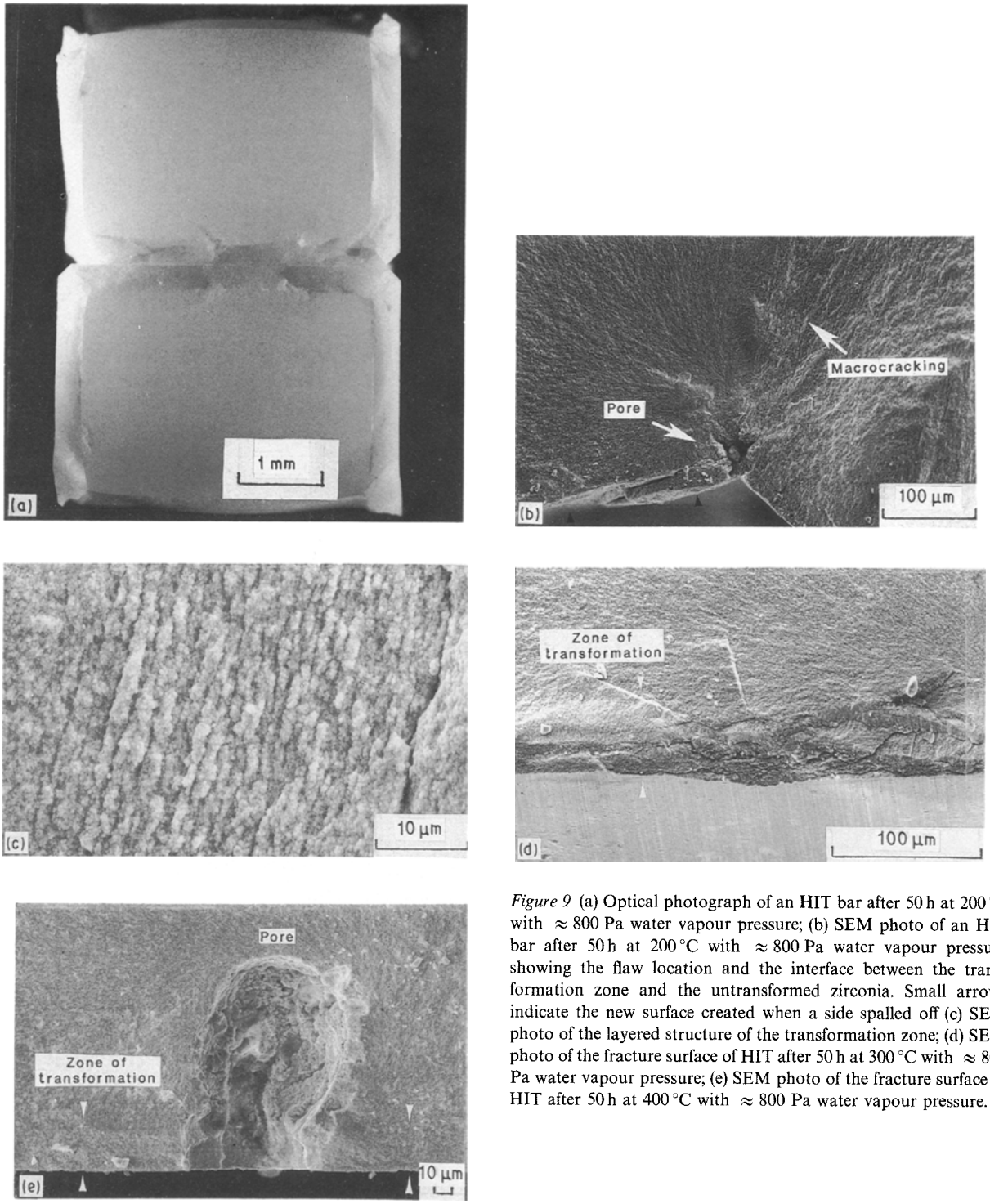

Figure 9 (a) Optical photograph of an HIT bar after 50 h at 200 °C with ≈ 800 Pa water vapour pressure; (b) SEM photo of an HIT bar after 50 h at 200 °C with ≈ 800 Pa water vapour pressure showing the flaw location and the interface between the transformation zone and the untransformed zirconia. Small arrows indicate the new surface created when a side spalled off (c) SEM photo of the layered structure of the transformation zone; (d) SEM photo of the fracture surface of HIT after 50 h at 300 °C with ≈ 800 Pa water vapour pressure; (e) SEM photo of the fracture surface of HIT after 50 h at 400 °C with ≈ 800 Pa water vapour pressure.

The KH material shows a very small transformation zone of 10–20 μm after the 200 and 300 °C treatments but no discernible zone after the 400 °C treatment. Examination of the fracture surfaces after the 400 °C treatment indicates that the inherent flaws now dominate.

Fractography of the NGK and KS TZPs showed no signs of a zone of transformation after any of the treatments. Furthermore, the same flaw types limit the as-received strength and the post heat treatment strengths.

4. Discussion

From the results reported here and those previously referenced, the surface layers seen during fractographic analysis are clearly m–ZrO_2 which has transformed from t–ZrO_2 as a result of the heat treatments. The divergent performance of these TZPs after exposure to low temperatures in the presence of water vapour can be summarized by examining the grain size and yttria content of each. Several references [2, 4, 6–9, 11, 16] have shown that an increase in the yttria content, a decrease in the grain size or a combination of both, will result in a TZP with superior resistance to low temperature degradation.

Lange reported that the retention of the tetragonal phase during *processing* is dependent on a combination of grain size and yttria content [20]. By plotting the grain size against the mol % yttria, he was able to

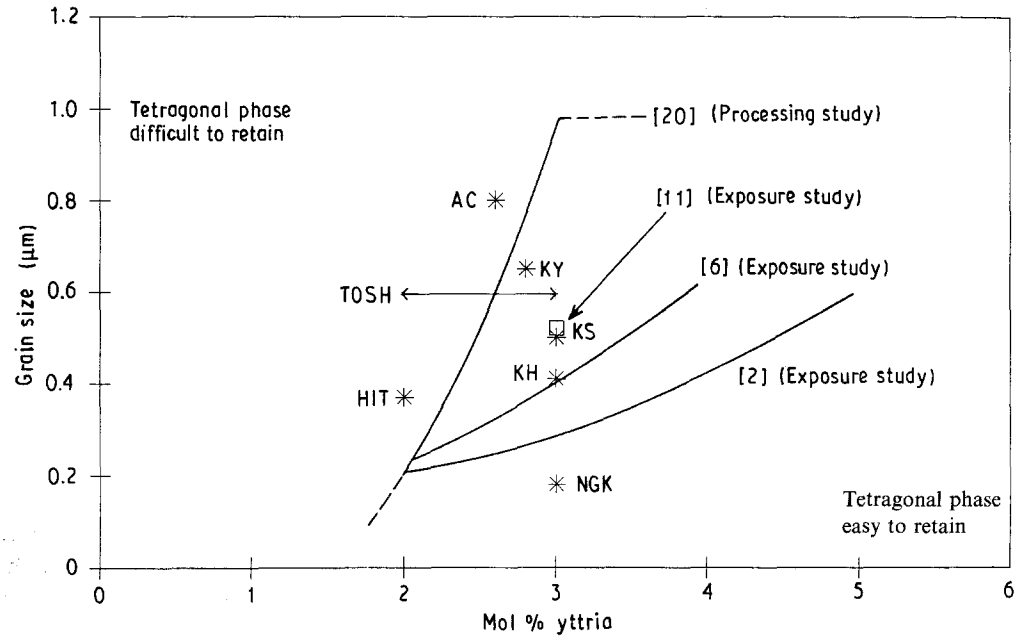

Figure 10 Grain size against mol % yttria for the seven TZPs examined in this study and data from [20, 2, 6, 11]. The curves approximate the boundary between the ability to retain the tetragonal phase. Data from the present study is shown as points for comparison.

define a critical grain size (D_c) necessary for the retention of $> 90\%$ of the tetragonal phase for a given yttria content during normal processing. The general trend is that as the amount of yttria additive decreased, so must D_c. Above D_c for a given yttria content the retention of the tetragonal phase becomes increasingly more difficult. The same relationship also seems to apply to the low temperature degradation phenomenon [2, 6, 11]. Fig. 10 summarizes the data from these investigations. The addition of the data from the seven TZPs examined in this study to Fig. 10 yields a general idea of how each TZP will fair when subjected to low temperature exposure in the presence of water vapour.

Due to the large number of TZPs evaluated, each will be discussed individually.

4.1. Toshiba (TOSH)

Underwent catastrophic degradation (complete loss of structural integrity) due to extensive macrocracking. This macrocracking enabled the water vapour to penetrate deep into the bulk resulting in a large zone of m–ZrO_2 and a significant reduction in properties. The degradation was the most severe of any of the TZPs examined.

The company literature shows that the TOSH TZP can have a yttria content ranging from 2.0–3.0 mol%. Due to the severity of the degradation and the large grain size, the yttria content in this batch was probably closer to the 2.0 mol % end of the range. In order to increase the resistance to this degradation, changes must be made in the processing of the material. An adjustment of the sintering schedule to reduce the possibility of grain growth, the use of hot pressing or hot isostatic pressing techniques, would appear to be appropriate. Also maintaining a yttria content closer to 3.0 mol % may also increase the resistance.

4.2. AC sparkplug (AC)

Although the "B" bars survived this exposure the catastrophic degradation of the smaller "A" bars indicates that this material has a low temperature degradation problem. Had the exposure conditions been more severe it is possible that the "B" bars would have also degraded catastrophically. Again, the degradation was the result of extensive macrocracking and the associated $t \rightarrow m$ transformation.

A change in the processing schedule to reduce the grain size, either by adjusting the sintering schedule or switching to hot pressing or hot isostatic pressing, is obviously needed. A minor increase in the yttria content may also help, but it is believed that the former would have more impact on the resistance to degradation.

4.3. Kyocera (KY)

As was the case with the above materials, this TZP also experienced catastrophic degradation of all but 2 bars. The mechanisms of degradation were the same as the TOSH and AC TZPs. Although the 2 bars survived, the properties were significantly reduced. Changes in the processing schedule or technique, as described above, would appear to have the most impact on improving the resistance to low temperature degradation since the yttria content is almost 3.0 mol %.

4.4. Hitachi (HIT)

Degradation and significant property losses occurred after all the treatments, but the most severe losses came only after the 200 °C treatment. The degradation was in the form of thermal spalling. It is possible that this spalling would have occurred at the other treatment temperatures if the exposure time and/or water

vapour pressure was increased, but further testing would be required to confirm this. Since the HIT is produced by hot pressing and it already has a very fine grain size, it is unlikely that changes in the processing would be sufficient to reduce the effects of this phenomenon. Rather, an increase in the yttria content would appear to be more beneficial.

4.5. Koransha HIPed (KH)

No physical degradation was observed but the properties were reduced after all three treatments. The most severe loss was after the 200 °C treatment. If the treatment conditions were more severe these losses may have been larger. Since the yttria content is 3.0 mol % it appears that only minor adjustments in the processing schedule would be necessary to reduce the grain size and possibly eliminate the effects of low temperature degradation.

4.6. Koransha sintered (KS)

As was the case with its counterpart, KH, no physical degradation was observed and the most significant property degradation occurred after the 200 °C treatment. Again changes in the sintering schedule would appear to be enough to reduce the grain size and effectively eliminate this degradation.

4.7. NGK-Locke (NGK)

No physical or property degradation was seen. Since this TZP is significantly below the curves in Fig. 10, it is expected that the material would still be very resistant to low temperature degradation even if the severity of the treatment conditions were increased.

The final three TZPs (KH, KS and NGK) are in excellent agreement with the findings [2, 6, 11] for TZPs containing 3.0 mol % yttria.

The present work and the studies referenced show that a fine-grained microstructure is important if a Y–TZP material is to resist low temperature degradation between 200 and 400 °C. However, previous work by the author [19], on these same Y–TZPs, showed that the fine-grained Y–TZPs have lower fracture toughness values than their coarse-grained counterparts. (The exception to this is NGK which has a relatively high toughness due to microstructural tailoring.) As a result, this trade-off between resistance to low temperature degradation and fracture toughness must be considered when examining a Y–TZP for structural applications.

5. Conclusions

1. The first five general observations outlined in the Introduction were confirmed. In particular, there was a strong relationship between degradation, grain size and yttria content. The final one was not observed since none of the TZPs were exposed to low temperatures in the absence of water or water vapour.

2. The NGK TZP was completely unaffected by the low temperature treatments in the presence of water vapour.

3. The KS and KH TZPs were affected by the treatments, the m–ZrO_2 content increased and the properties decreased slightly, but the extent of degradation was minimal.

4. The HIT TZP had significant degradation after the 200 °C treatment due to spalling of the sides of the bar. This effect was not present when the treatment temperature increased.

5. Three TZPs (TOSH, AC and KY) experienced catastrophic degradation after all treatments due to the spontaneous tetragonal-to-monoclinic transformation.

Acknowledgement

Research was sponsored by the US Department of Energy, Assistant Secretary for Conservation and Renewable Energy, Office of Transportation Systems, as part of the Ceramic Technology for Advanced Heat Engines Project of the Advanced Materials Development Program, under contract DE-AI05-840R21411 with Martin Marietta Energy Systems, Inc.

The author wishes to acknowledge the efforts of David Quinn at AC Sparkplug, Flint, MI who performed the treatments and provided helpful discussions and insight during the course of this study.

References

1. K. KOBAYASHI, H. KUWAJIMA and T. MASAKI, *Solid State Ionics* **3** (1981) 489.
2. M. WATANABE, S. IIO and I. FUKUURA, in "Advances in ceramics, science and technology of Zirconia II, Vol. 2, edited by N. Claussen, M. Rühle and A. H. Heuer (The American Ceramic Society, Columbus, Ohio, 1984) p. 391.
3. K. NAKAJIMA, K. KOBAYASHI and Y. MURATA, *ibid.* p. 399.
4. T. SATO and M. SHIMADA, *J. Amer. Ceram. Soc.* **67** (1984) C-212.
5. *Idem., ibid.* **68** (1985) 356.
6. T. SATO, S. OHTAKI and M. SHIMADA, *J. Mater. Sci.* **20** (1985) 1466.
7. F. F. LANGE, G. L. DUNLOP and B. I. DAVIS, *J. Amer. Ceram. Soc.* **69** (1986) 237.
8. A. J. A. WINNBST and A. J. BURGGARAAF, in "Advances in ceramics, science and technology of Zirconia III", edited by S. Somiya, N. Yamamoto and H. Hanagida (The American Ceramic Society, Columbus, Ohio, 1988) p. 39.
9. S. SCHMAUDER and H. SCHUBERT, *J. Amer. Ceram. Soc.* **69** (1986) p. 534.
10. M. YOSHIMURA, T. NOMA, K. KAWABATA and S. SOMIYA, *J. Mater. Sci. Lett.* **6** (1987) p. 465.
11. H. Y. LU and S. Y. CHEN, *J. Amer. Ceram. Soc.* **70** (1987) 537.
12. T. SATO, S. OHTAKI, T. ENDO and M. SHIMADA, in "High tech. ceramics", edited by P. Vincenzini (Elsevier Science Publishers, Amsterdam, 1987) p. 281.
13. M. YOSHIMURA, T. NOMA, K. KAWABATA and S. SOMIYA, *J. Ceram. Soc. Jpn. Inter. Ed.* **96** (1988) 263.
14. T. SATO, S. OHTAKI, T. ENDO and M. SHIMADA, *J. Amer. Ceram. Soc.* **68** (1985) C-320.
15. T. SATO and M. SHIMADA, *Amer. Ceram. Soc. Bull.* **64** (1985) 1382.
16. *Idem.*, in "Ceramic materials and components for engines", edited by W. Bunk, and H. Hausner (Deutsche Keramische Gesselschaft, Germany, 1986) p. 291.
17. T. SATO, S. OHTAKI, T. ENDO and M. SHIMADA, in "Advances in ceramics, science and technology of Zirconia

III", Vol. 24, edited by S. Somiya, N. Yamamoto, and H. Hanagida, (The American Ceramic Society, Columbus, Ohio, 1988) p. 501.
18. L. J. SCHIOLER, U.S. Army Materials Technology Laboratory, MTL TR 87-29, prepared for Oak Ridge National Laboratory for U.S. Department of Energy under Interagency Agreement DE-A105-84OR21411, June 1987.
19. J. J. SWAB, U.S. Army Materials Technology Laboratory, MTL TR 89-21, prepared for Oak Ridge National Laboratory for U.S. Department of Energy under Interagency Agreement DE-A105-87OR21411, March 1989.
20. F. F. LANGE, *J. Mater. Sci.* **17** (1982) 240.

Received 24 May 1990
and accepted 31 January 1991